Electromagnetic transitions in ^{30}Al

R. L. Kozub, C. B. Chitwood,* and D. J. Fields*
Department of Physics, Tennessee Technological University, Cookeville, Tennessee 38505

C. J. Lister,† J. W. Olness, and E. K. Warburton
Brookhaven National Laboratory, Upton, New York 11973
(Received 25 August 1983)

Deexcitation γ rays of ^{30}Al following the ^{14}C(^{18}O,pn)^{30}Al fusion-evaporation reaction have been observed in singles, in coincidence with the evaporated protons, and in coincidence with other γ rays in cascade. Gamma-ray yield curves were measured over the ^{18}O beam energy range 15–35 MeV. Angular distributions of γ rays observed in coincidence with protons at 0° were measured for four transitions. Limits on level lifetimes were determined, and no evidence for a long-lived isomeric transition was found. Excitation energies deduced are, in keV: 0, 243.90(8), 687.53(12), 991.0(9), 1118.7(7), and 1245.6(8). Corresponding spins and parities are 3^+, $(1,2)^\pm$, 1^+, $(2,3,4,)^\pm$, $(1,2,3)^\pm$, and $(4)^\pm$, respectively. The results are compared to recent shell model calculations.

[NUCLEAR REACTIONS ^{14}C (^{18}O,pnγ)^{30}Al, $E(^{18}\text{O})=15$–35 MeV; measured $I_\gamma(E,\theta)$, E_γ; pγ coin; $\gamma\gamma$ coin; deduced decay scheme, limits on τ, probable J.]

I. INTRODUCTION

Neutron-rich nuclei in the lower *sd* shell present a challenge to even the most up-to-date theoretical models of nuclear structure. This is particularly true for odd-odd nuclei, such as ^{30}Al. Excitation energies for low-lying levels in ^{30}Al have been measured by Ajzenberg-Selove and Igo[1] via the ^{30}Si(t,^{3}He)^{30}Al reaction. They assumed that the level they observed at 250±30 keV excitation is an isomer, and that its decay is responsible for the long-lived activity ($\tau_{1/2}=72.5\pm1.3$ s) reported by Peeters.[2] In a study of the $A=30$ β-decay chain, Détraz *et al.*[3] observed γ-ray transitions which they assigned to the deexcitation of ^{30}Al levels at 243 and 685 keV. They also deduced spin and parity assignments for the ground state (3^+) and 685-keV level (1^+). However, apart from a preliminary report on the present work,[4] no other information on the excited states of ^{30}Al is available. We have employed the ^{14}C(^{18}O,pnγ)^{30}Al reaction to measure excitation energies and lifetime limits for five excited states of ^{30}Al. In addition, proton-gated γ-ray angular distributions were measured for four of these states.

II. EXPERIMENTAL METHODS

In order to unambiguously identify levels in ^{30}Al and to investigate their decay properties, three types of measurements, all utilizing the ^{14}C(^{18}O,pnγ)^{30}Al reaction, were made:

(1) γ-ray yields in singles and in coincidence with evaporated protons were measured as a function of ^{18}O beam energy;

(2) γ-γ coincidences were recorded;

(3) angular distributions of γ rays were measured in coincidence with forward-emitted protons.

Detailed descriptions of the experimental procedures used for these measurements are given below.

The experimental arrangement used to acquire γ-γ coincidence data is illustrated in Fig. 1. A 25-MeV ^{18}O beam bombarded a 106-μg/cm^2 ^{14}C target deposited on a 2-mg/cm^2-thick Ni backing. The ^{18}O beam and heavy recoiling ions were stopped in a 40-mg/cm^2-thick Ta foil clamped onto the downstream (Ni) side of the target. Gamma rays were detected with *n*-type high-purity Ge (*n*HPGe) detectors having relative efficiencies of 13% and 20% placed at 90° and 55° to the beam direction, respectively. The distance from each *n*HPGe crystal to the target was 43 mm. Lead collimators of 12.5-mm thickness

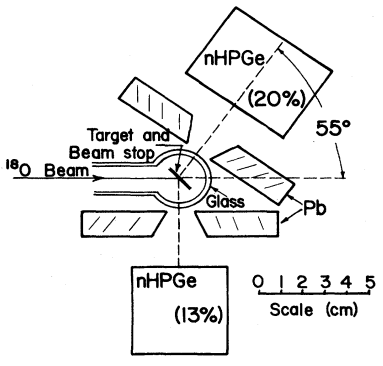

FIG. 1. Experimental setup for γ-γ coincidence and γ-ray singles yield curve measurements.

were used to reduce the false coincidence events arising from a single γ-ray scattering between the two detectors. The timing resolution achieved was approximately 15 ns FWHM. Signals from the two γ-ray detectors and the time-to-amplitude converter (TAC) were stored in event mode on magnetic tape.

Singles yield curve data were acquired using an escape suppression spectrometer with the *n*HPGe detector operated inside a NaI(Tl) anticoincidence shield. The target-beam stop arrangement was similar to that described above for γ-γ coincidences. In this arrangement, an evacuated space, a few microns in thickness, existed between target backing and stopper. This resulted in fully-Doppler-broadened line shapes for prompt γ-ray transitions, and narrow line shape components, characteristic of the *n*HPGe-detector resolution, only for relatively long-lived ($\tau \gtrsim 1$ ps) decays. Thus, most prompt and delayed components were easily separable in the spectra, allowing the extraction of yield curves for both prompt and β-delayed γ rays. Beam current integration was used to normalize all yield curve data.

The setup for acquiring particle-γ ray coincidence data is shown in Fig. 2. Beams of ^{18}O projectiles, accelerated to energies ranging from 15 to 35 MeV, bombarded a 103-μg/cm^2-thick ^{14}C target deposited on a Au backing of approximately 7-mg/cm^2 thickness. This thickness of Au was sufficient to stop heavy evaporation residues having $A \sim 30$. The beam and ^{14}C recoils were stopped in a 20-mg/cm^2-thick Ta foil placed between the target and the particle counter telescope, as shown in Fig. 2. The telescope consisted of 50-μm$\times$100-mm^2 and 1000-μm$\times$300-mm^2 silicon surface-barrier detectors for the ΔE and E counters, respectively, placed such that particles emitted within approximately $\pm 29°$ of the beam direction could be detected. Most of the light particles had enough energy to penetrate both the Au backing and the Ta foil, and were thus eligible for detection via the telescope. The low-energy threshold for detection and identification of protons was approximately 2 MeV.

Gamma rays were detected with an *n*HPGe detector of 20% relative efficiency. Gamma-ray spectra were acquired both in singles and in coincidence with various particle groups observed in the ΔE-E map, on which two-dimensional gate regions were set at the beginning of the experiment. Yield curve measurements were taken with the front face of the Ge crystal at 54 mm from the target and positioned at $\theta_\gamma = 115°$ (see Fig. 2). Angular distributions were measured at 25-MeV beam energy with the Ge crystal at 97 mm from the target. Detector attenuation coefficients were estimated to be $Q_2 = 0.96$ and $Q_4 = 0.87$ for this geometry over the γ-ray energy range of interest.[5] Data were acquired at four laboratory angles: $\theta_\gamma = 0°$, 105°, 125°, and 145°. These angles were cycled a total of four times, with approximately 2 h of data accumulation per angle per cycle. The total number of charged particles detected was used as a normalization basis for each run. The angular variation of the attenuation of γ radiation by the target chamber and counter telescope assembly was measured as a function of γ-ray energy using a ^{152}Eu source placed at the target position. Spectra were also acquired at 25-MeV beam energy and $\theta_\gamma = 115°$ using a 100-

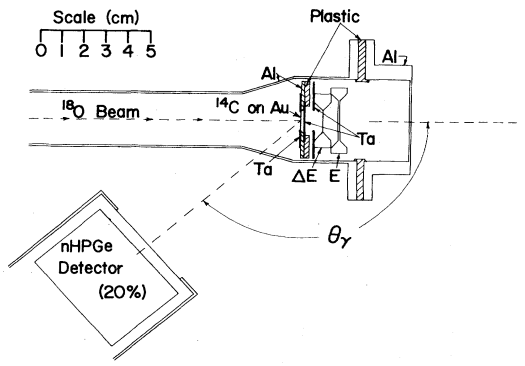

FIG. 2. Experimental setup for particle-γ coincidence measurements.

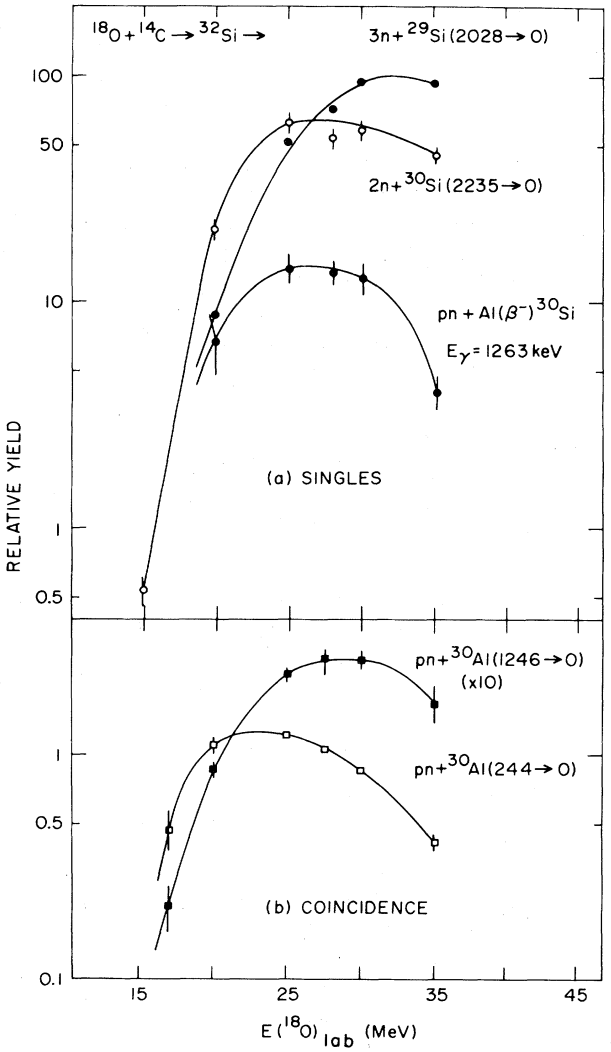

FIG. 3. Relative yields of various γ-ray transitions (a) in singles and (b) in coincidence with protons, for ^{18}O+^{14}C reactions, vs ^{18}O laboratory energy. Errors are statistical only, and curves are drawn to guide the eye.

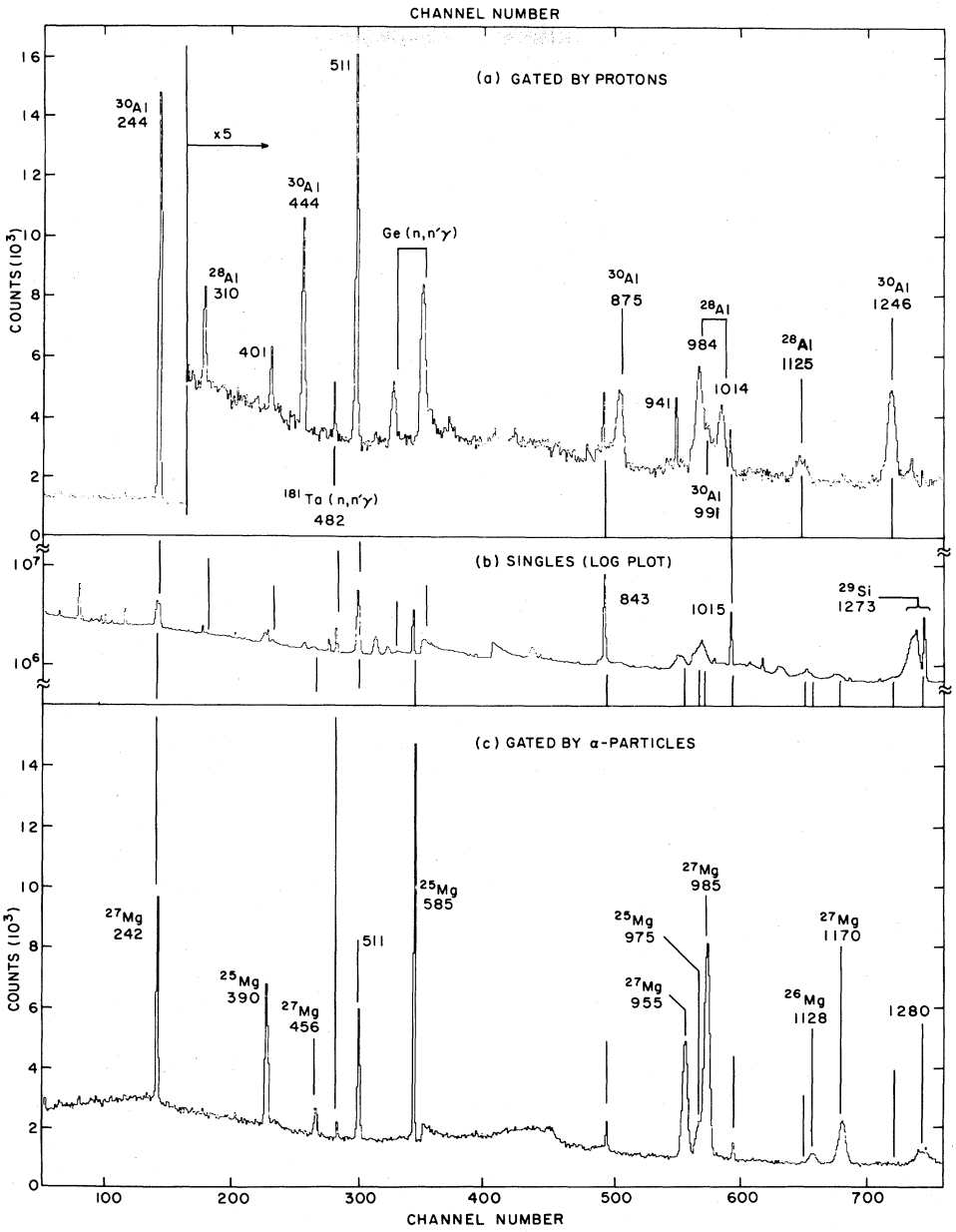

FIG. 4. Spectra of γ rays from $^{18}O+^{14}C$ reactions acquired (a) in coincidence with protons, (b) in singles, and (c) in coincidence with α particles. Data have been adjusted to the same energy gain. The 242- and 244-keV lines were clearly resolved in a singles spectrum taken with twice the conversion gain of the one shown here.

μg/cm^2 ^{12}C target on an 8-mg/cm^2 Au backing, in order to identify γ rays originating from the natural carbon contamination on the ^{14}C target. These experiments were rather sensitive to even small amounts of contamination, owing to the relatively large cross section for charged particle emission from reactions of the beam with ^{12}C, as compared to that from reactions with ^{14}C.

III. RESULTS AND DISCUSSION

Some of the yield curve data taken in singles and in coincidence with protons are shown in Fig. 3. Spectra obtained by gating on protons and on α particles are compared to a singles spectrum in Fig. 4. As is apparent from Fig. 4(a), the ^{30}Al 991-keV line is partially obscured by the 984- and 1014-keV lines of ^{28}Al, formed primarily via the pn-evaporation channel following reactions of the ^{18}O projectiles with the ^{12}C contamination on the target. The 991-keV line was not present in spectra obtained using the ^{12}C target, and is interpreted as the decay to ground state of an ^{30}Al level reported tentatively in Ref. 1 at 1.00$\pm$0.03 MeV. Properly normalized spectra taken with the ^{12}C target were subtracted from those taken with the ^{14}C target, and the resultant spectra were used to determine centroids

for the 991-keV transition. The γ-γ coincidence data showed both the 444- and 875-keV lines to be in coincidence with the 244-keV transition. The ^{30}Al levels and decay scheme deduced in the present work are compared in Fig. 5 to the (t, ^{3}He) results of Ref. 1 and to the shell model calculations of Wildenthal.[6] It should be noted that, if the excitation energies of Ref. 1 are multiplied by the constant factor 0.986, then the energies from the (t, ^{3}He) reaction and those measured in the present work agree within ± 4 keV. The relative side-feeding intensity to the ^{30}Al ground state was determined by measuring the relative strengths of β-delayed γ rays from ^{30}Si.

A summary of experimental results is given in Tables I and II. Gamma-ray energies were determined using standard calibration sources, and Doppler-shift corrections were applied by measuring centroids at each of the four angles for which angular distribution data were taken. The fractional Doppler shifts [$F(\tau)$] extracted were converted to level lifetimes using Doppler shift attenuation (DSA) calculations based on the method of Blaugrund.[7] The experimental determination of the initial ^{30}Al recoil velocity was based primarily on the assumption of a full Doppler shift for the short-lived ($\tau \approx 30$ fs) 2272$\rightarrow$0 transition in ^{30}Al, which was observed simultaneously via the parallel reaction ^{12}C(^{18}O,pnγ)^{28}Al. Several other fast transitions, including several others in ^{28}Al, provided supporting data. After correction for the ^{12}C$-^{14}$C mass difference, the experimentally-determined value of $\beta = 0.0275(20)$ is in satisfactory agreement with kinematics calculations in which the evaporated proton is moving forward in the center-of-mass frame.

The lifetime of the 244-keV level has been corrected for feeding from the 688-keV level, but no other significant feeding data are known, so corrections were not applied in any of the other cases. The errors given do not account for unknown feeding. Time spectra from γ-γ coincidence data associated with the 688$\rightarrow$244$\rightarrow$0 cascade were examined to investigate the possibility that the 244-keV state is a long-lived isomer, as suggested by Ajzenberg-Selove and Igo.[1] It was found that $\tau < 12$ ns, i.e., no retardation of the 244$\rightarrow$0 decay was perceived within the electronic limits of our experiment.

As is apparent from the angular distributions shown in Fig. 6 and the large errors on the Legendre coefficients (Table I), the data for each of the four transitions in question are consistent with a pure dipole interpretation; our statistical uncertainties are too large to be any more definitive. The uncertainties on the a_4 coefficients are particularly large if the data are fitted by varying three parameters. Thus, the a_2 values deduced from a two-parameter fit, with a_4 fixed at zero, are also shown in Table I as a_2'. These two-parameter fits are represented by dashed lines in Fig. 6.

The spin and parity assignments shown in Fig. 5 were deduced by considering our experimental results in conjunction with some general properties of fusion-evaporation reactions,[8] and with angular momentum properties of electromagnetic decay.[9] Fusion-evaporation reactions most strongly populate the yrast states, which usually decay via "stretched" cascades of nearly pure multipoles of order L, where $L = J_i - J_f$, and $J_i > J_f$. Stretched dipole transitions typically have angular distribution coefficients of $a_2 \approx -(0.2\text{–}0.3)$, while stretched quadrupole transitions have $a_2 \approx +(0.1\text{–}0.2)$ and $a_4 \simeq -(0.05\text{–}0.1)$. The observed strong side feeding of the ground state ($J^\pi = 3^+$) and the 1246-keV state, and the apparent single decay branch of the latter to the ground state, seem to fit this yrast decay pattern if the 1246-keV state has $J = 4$. As further support of this assignment, the 1246$\rightarrow$0 transition has a_2 (or a_2') near the above-mentioned range for stretched dipoles (see Table I). Assuming this is a pure dipole transition, the strength would be $|M(M1)|^2 = 0.097(46)$ Weisskopf units (W.u.)[10] or $|M(E1)|^2 = 3.1(1.5) \times 10^{-3}$ W.u., depending on wheth-

TABLE I. Experimental data for transitions in ^{30}Al observed via the ^{14}C(^{18}O,pnγ)^{30}Al reaction. Uncertainties in the least significant figures are given in parentheses.

Energies (keV)			BR	Legendre coefficients[a]				
E_i	E_f	E_γ	(%)	a_2 (%)	a_4 (%)	a_2' (%)	$F(\tau)$[b]	τ (ps)[b]
244	0	243.90(8)	100	−12(3)	−3(3)	−14(2)	<0.05	12000 > τ > 4.0
688	0	687.5[c,d]	<5[d]					
	244	443.63(8)	>95	+7(11)	−8(11)	+4(8)	0.25(5)	1.0(3)
991	0	991.0(9)	(100)				0.76(11)	0.14(8)
1119	244	874.8(6)	>96	+19(15)	+3(16)	+20(11)	0.79(12)	0.12(8)
	688	431.2[c]	<4					
1246	0	1245.6(8)	(100)	−11(9)	−6(10)	−13(6)	0.71(11)	0.17(8)

[a]Coefficients a_2 and a_4 are from fitting angular distribution data by varying three parameters. Coefficients a_2' are from fitting data with a_4 fixed at zero.

[b]These results establish lower limits on $F(\tau)$ and correspondingly upper limits on τ for all but the 244$\rightarrow$0 transition, owing to the unknown feeding times. The $F(\tau)$ value for the latter was corrected for feeding from the 688-keV level.

[c]The transition energy was calculated as $E_i - E_f$, but was not observed experimentally.

[d]A weak 684.6(1.3)$\rightarrow$0 decay branch (4%) was reported in Ref. 3.

TABLE II. Comparison of experimental results with results from shell-model calculations. Experimental uncertainties in least significant figures are indicated in parentheses.

Energies (keV)		Assumed	BR	Transition strength (W.u.) Expt.[b,c]	Theory		τ (ps)	
E_i	E_f	$J_i \rightarrow J_f$[a]	(%)	$M1$	$M1$	$E2$	Expt.[b]	Theory[d]
244	0	$2_1 \rightarrow 3_1$	100	$0.0002 < \lvert M(M1) \rvert^2 < 0.55$	0.090	4.3	$4.0 < \tau < 12000$	24.
688	0	$1_1 \rightarrow 3_1$	<5			2.9		
	244	$1_1 \rightarrow 2_1$	>95	0.36(11)	0.39	5.3	1.0(3)	0.94
991	0	$4_1 \rightarrow 3_1$	(100)	0.23(13)[e]	0.14	5.8	0.14(8)	0.22
	244	$4_1 \rightarrow 2_1$				0.11		
1119	0	$3_2 \rightarrow 3_1$			0.061	2.8		
	244	$3_2 \rightarrow 2_1$	>96	0.40(26)[f]	0.35	3.7	0.12(8)	0.10
	688	$3_2 \rightarrow 1_1$	<4			1.6		
1246	0	$4_1 \rightarrow 3_1$	(100)	0.097(46)[g]	0.14	5.8	0.17(8)	0.11
	244	$4_1 \rightarrow 2_1$				0.11		

[a]Spins are those assumed for comparison with theoretical calculations for positive-parity states, and are not assignments (see the text and Fig. 5). Spin assignments from Ref. 3 are used for the ground state and the 688-keV level.

[b]Except for the 244→0 transition, no corrections for possible feeding have been applied (see the text).

[c]Experimental $E2$ transition strengths are not given, since mixing ratios were not measured and none of the observed transitions are predominantly quadrupole (see the text). $M1$ strengths shown were determined assuming all transitions are purely dipole.

[d]See Ref. 6.

[e]If the 991-keV state has negative parity, the $E1$ transition strength is $(7.4\pm4.2)\times10^{-3}$ W.u.

[f]If the 1119-keV state has negative parity, the $E1$ transition strength is $(13\pm8)\times10^{-3}$ W.u.

[g]If the 1246-keV state has negative parity, the $E1$ transition strength is $(3.1\pm1.5)\times10^{-3}$ W.u.

er the 1246-keV level has positive or negative parity, respectively.

The other excited states are fed relatively weakly (Fig. 5), and are thus probably not part of a yrast cascade. The angular distribution for the 688→244 transition is essentially flat (Fig. 6), and is thus consistent with the low spin assignment ($J^\pi = 1^+$) made by Détraz *et al.*,[3] for the 688-keV level. The lifetime measured for the 688→244 decay would demand that the transition be predominatenly di-

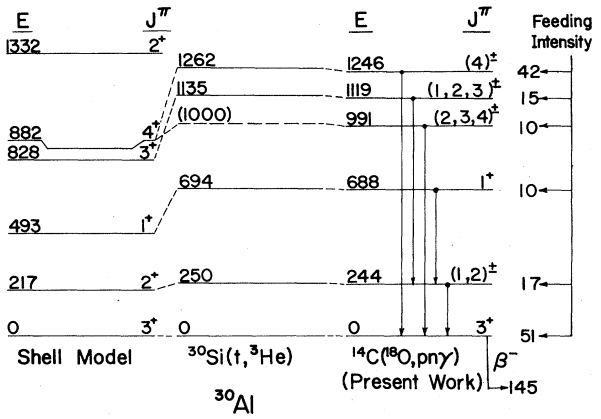

FIG. 5. Energy level diagram for ^{30}Al, comparing shell-model calculations (Ref. 6) and (t, ^{3}He) results (Ref. 1) with present work and the results of Ref. 3. Assumed level correspondences are shown by dashed lines (see the text and Table II). Experimental errors in energies of Ref. 1 range from 15 to 30 keV. The experimental spin and parity assignments are those assigned in Ref. 3 and suggested via present results.

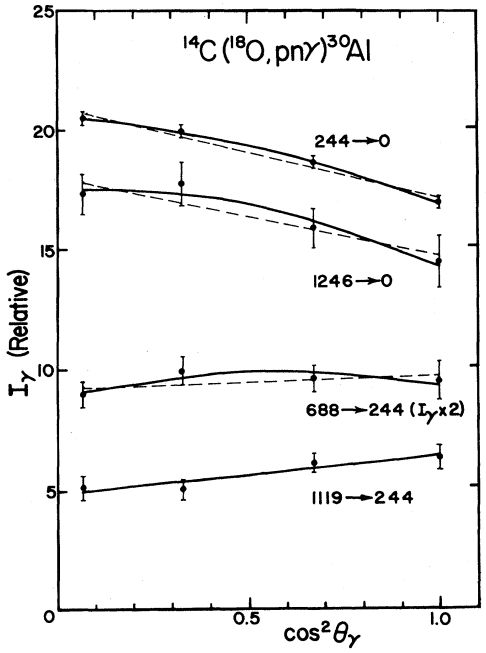

FIG. 6. Angular distributions of γ-ray transitions in ^{30}Al. The errors are statistical. Data as shown are not corrected for detector efficiency. Solid curves are least-squares fits to the equation

$$I_\gamma = A_0[1 + a_2 Q_2 P_2(\cos\theta_\gamma) + a_4 Q_4 P_4(\cos\theta_\gamma)] .$$

Dashed lines are fits with a_4 fixed at zero. See the text and Table I for further details.

pole; if it were a pure $E2$ transition, its strength would be 8500(2600) W.u., far in excess of the accepted limit.[11] On this basis, the spin of the 244-keV state is restricted to 0, 1, or 2. Further, the anisotropy of the 244→0 transition rules out $J=0$. Thus, we conclude $J^{\pi}=(1,2)^{\pm}$ for the 244-keV level. The limit on its lifetime ($\tau<12$ ns) would imply $|M(E2)|^2>14$ W.u. if $J=1$, which is not unreasonable. A better lifetime measurement, for which the recoil distance method (RDM) would seem appropriate, would help to determine which of the spin-parity alternatives is correct.

The lifetimes of the 991- and 1119-keV states would imply that both the 991→0 and 1119→244 transitions are also predominantly dipole; again, the pure $E2$ strengths required—1100(600) W.u. and 2400(1600) W.u., respectively—would be unacceptably large. The 1119→244 transition is anisotropic.[12] Thus, $J=(2,3,4)$ for the 991-keV level and (1,2,3) for the 1119-keV state.

IV. COMPARISON TO SHELL MODEL CALCULATIONS

Experimental transition strengths and lifetimes are compared with those from the Wildenthal shell model calculations[6] in Table II. Initial and final spins of experimental levels were assumed which are consistent with the conclusions drawn in the previous section and with the previous assignments in Ref. 3 for the ground and 688-keV states, and which seemed reasonable in light of the level order predicted via the model (Fig. 5). Only $M1$ experimental transition strengths, calculated by assuming pure dipole transitions, are listed. Similar calculations of $E2$ strengths, assuming pure quadrupole transitions, would imply strengths in excess of the acceptable upper limit of 100 W.u. for all but the 244→0 transition, for which $|M(E2)|^2>14$ W.u.

The calculated $M1$ strengths and lifetimes all agree with the corresponding experimental values, within experimental uncertainties. Thus, the identification with shell-model states shown in Fig. 5 is probably not unreasonable. However, an interesting puzzle is posed by the 991- and 1246-keV states, both of which decay exclusively to the ground state. As illustrated in Table II, either of them could be interpreted as corresponding to the predicted 4_1^+ state at 882 keV (Fig. 5). Neither of them has the decay properties of the predicted 2_2^+ state at 1332 keV, as this state should also have a strong (~40%) branch to the 2_1^+ state, which presumably corresponds to the 244-keV state observed experimentally. It would thus appear that either the 991- or the 1246-keV state has negative parity,[6] arising from the coupling of the unpaired *sd*-shell proton to the unpaired neutron in an *fp* orbital. Model calculations for negative parity states of ^{30}Al have not yet been performed; the results should be interesting.

As a final note, the model predicts the 1_2^+ state to lie at an excitation energy of 2139 keV. The decay energy of this level to the ground state or first excited state would be in reasonable agreement with the energy of 2165 keV measured by Détraz *et al.*[3] for a weak γ-ray transition in the $A=30$ β-decay chain.

V. SUMMARY AND CONCLUSIONS

The γ-ray decay properties of five excited states of ^{30}Al have been investigated. Shell-model calculations, performed by Wildenthal for positive-parity states, are in good agreement with experimental results. It would appear that either the 991- or 1246-keV level, but probably not both, has negative parity. Spin and parity assignments suggested for other states are summarized in Fig. 5. No evidence was found for the long-lived isomeric state discussed in Refs. 1 and 2.

ACKNOWLEDGMENTS

M. R. Bynum, T. L. Matthews, S. G. Menees, and T. J. Theiss (all of TTU) assisted in data acquisition and/or analysis. The visitors from TTU appreciate the hospitality and assistance provided by the BNL tandem laboratory staff. The authors are grateful to B. H. Wildenthal of Michigan State University for providing results of shell-model calculations prior to publication. This research was supported by the U.S. Department of Energy under Contracts No. DE-AS05-79ER10335 (TTU) and DE-AC02-76H00016 (BNL).

*Present address: National Superconducting Cyclotron Laboratory, Michigan State University, East Lansing, MI 48824.

†Present address: Department of Physics, University of Manchester, Manchester, M13 9PL, United Kingdom.

[1] F. Ajzenberg-Selove and G. Igo, Phys. Rev. 188, 1813 (1969).

[2] E. Peeters, Phys. Lett. 7, 142 (1963).

[3] C. Détraz, D. Guillemaud, G. Huber, R. Klapisch, M. Langevin, F. Naulin, C. Thibault, L. C. Carraz, and F. Touchard, Phys. Rev. C 19, 164 (1979).

[4] C. B. Chitwood, D. J. Fields, R. L. Kozub, J. W. Olness, E. K. Warburton, and C. J. Lister, Bull. Am. Phys. Soc. 27, 497 (1982).

[5] K. S. Krane, Nucl. Instrum. Methods 98, 205 (1972).

[6] B. H. Wildenthal, private communication; see also W. Chung, Ph.D. thesis, Michigan State University, 1976 (unpublished).

[7] A. E. Blaugrund, Nucl. Phys. 88, 501 (1966).

[8] P. Gorodetzky, J. J. Kolata, J. W. Olness, A. R. Poletti, and E. K. Warburton, Phys. Rev. Lett. 31, 1067 (1973); A. M. Nathan, J. W. Olness, E. K. Warburton, and J. B. McGrory, Phys. Rev. C 16, 192 (1977).

[9] T. Yamazaki, Nucl. Data 3A, 1 (1967).

[10] S. J. Skorka, J. Hertel, and T. W. Retz-Schmidt, Nucl. Data 2A, 347 (1966).

[11] P. M. Endt, At. Data Nucl. Data Tables 23, 3 (1979).

[12] The positive a_2 values for the 1119→244 keV transition (Table I, Fig. 6) could be owing to poor spin alignment, as expected for a low-spin state [see, e.g., A. R. Poletti and E. K. Warburton, Phys. Rev. 137, B595 (1965)], and/or to quadrupole mixing.